

**First-principles study of the surfaces of zirconium during early stages of metal oxidation**

by

=====

Submitted to the Department of Nuclear Science and Engineering  
in partial fulfillment of the requirements for the degree of

Bachelor of Science in Nuclear Science and Engineering

at the

Massachusetts Institute of Technology

June 2015

© 2015 =====. All rights reserved.

The author hereby grants to MIT permission to reproduce  
and to distribute publicly paper and electronic  
copies of this thesis document in whole or in part  
in any medium now known or hereafter created.

Author .....  
Department of Nuclear Science and Engineering  
May 1, 2015

Certified by .....  
=====  
Professor, Nuclear Science and Engineering  
Thesis Supervisor

Accepted by .....  
Michael P. Short  
Professor of Nuclear Engineering  
Chairman, Department Committee on Undergraduate Students



# First-principles study of the surfaces of zirconium during early stages of metal oxidation

by

=====

Submitted to the Department of Nuclear Science and Engineering  
on May 1, 2015, in partial fulfillment of the  
requirements for the degree of  
Bachelor of Science in Nuclear Science and Engineering

## Abstract

The surfaces of zirconium during early stages of metal oxidation were examined by first-principles calculations using density functional theory. DFT calculations suggested that the interaction between the oxide and the substrate induced a slight vertical contraction of the oxide film and a slight buckling of the Zr layer in the oxide in which the latter effect was found to be more important. The total effect was significant. In fact, among the three examined configurations, the difference in heights across the oxide surface could reach 0.55 Å which should be visible under STM images. Therefore, the periodic relaxation patterns observed on the surface of zirconium at the initial stage in of its oxidation in previous study could be explained by the buckling of the zirconium layer in the oxide coupled with the fact that there was a mismatch between Zr metal and ZrO<sub>2</sub> oxide lattice parameters.

Thesis Supervisor: =====

Title: Professor, Nuclear Science and Engineering



# Acknowledgments



# Contents

<b>1</b>	<b>Introduction</b>	<b>13</b>
<b>2</b>	<b>Literature Background</b>	<b>15</b>
<b>3</b>	<b>Computational Methods, Results and Discussion</b>	<b>19</b>
3.1	Zirconium substrate modeling . . . . .	20
3.1.1	Zirconium bulk structure . . . . .	20
3.1.2	Zirconium surface structure . . . . .	23
3.2	Early phase of zirconium corrosion modeling . . . . .	24
<b>4</b>	<b>Conclusion &amp; Future Work</b>	<b>27</b>
	<b>Bibliography</b>	<b>29</b>



# List of Figures

2-1	STM images of zirconium surface at its early oxidation stage . . . . .	16
3-1	Zirconium Metal Bulk K-points convergence . . . . .	21
3-2	Regression fitting of DFT results to third-order Birch-Murnagahn equation of state . . . . .	22
3-3	A periodic slab that consisted of three zirconium layers separated by a vacuum region, which had a thickness equivalent to that of four bulk Zr layers. The rectangular box represents the actual computational supercell. . . . .	23
3-4	Zirconium/zirconia surface with ABCA stacking order . . . . .	25
3-5	Zirconium/zirconia surface with ABCB stacking order . . . . .	25
3-6	Zirconium/zirconia surface with ABCC stacking order . . . . .	25



# List of Tables

3.1	Comparison of the optimized Zr lattice parameters and bulk modulus to the reported experimental values . . . . .	22
3.2	Zirconium surface energies calculated in DFT. Comparison with experimental values is also given. . . . .	23



# Chapter 1

## Introduction

Zirconium alloys, Zircalloys, which consist of zirconium and other metals are of interest for many applications including electrolytes for advanced solid oxide fuel cells [1], corrosion-resistant coatings [2, 3] and structural materials for nuclear reactors [2]. In fact, since zircalloys are well-known for their exceptionally low absorption cross-section of thermal neutrons along with their great mechanical properties: high hardness, ductility and corrosion resistance, they are usually used in nuclear engineering as cladding of fuel rods in nuclear reactors. These alloys are pushed to endure harsher operation environment in the nuclear reactor, thus there is an absolutely need to understand the fundamental of their metal corrosion process, ultimately to ensure the safety of a nuclear reactor. It is well-known that the major player in longevity of a zirconium alloy cladding is the protective, electrically insulating layer of zirconium oxide ( $ZrO_2$ ) which natively covers zirconium alloy. Thus knowing the chemical and structural nature of the initial oxide formed on zirconium surfaces will be a major help in develop a framework to solve problems of relevance to the corrosion of zirconium alloys.



# Chapter 2

## Literature Background

In his latest work on initial surface oxide structure during early stages of zirconium oxidation, Ma reported to find a strange pattern appeared on STM images of his zirconium surface [22]. This pattern was shown in Fig.2-1. Ma suggested that the pattern could be of the growth of an ultra-thin layer of zirconia on top of zirconium metal. However, no further experiment results could be used to explain this pattern. In this situation, computational results from examination of this structure could be helpful.

Density Functional Theory (DFT) is a powerful atomistic modeling technique widely used in condensed-matter physics, computational physics, and computational chemistry. In general, DFT is extremely helpful at interpreting and predicting of complex system behavior at an atomic scale. In fact, DFT is specifically used in understanding materials that are highly sensitive to synthesis and processing parameters. For this reason, DFT is chosen to be the main atomistic modeling technique that would be used to model and simulate the two main materials in this study which are zirconium and its oxide, zirconia.

In the literature, many studies have tried to examine the properties of  $\text{ZnO}_2$  on different substrates to serve as models supporting for reforming catalysts and fuel cell

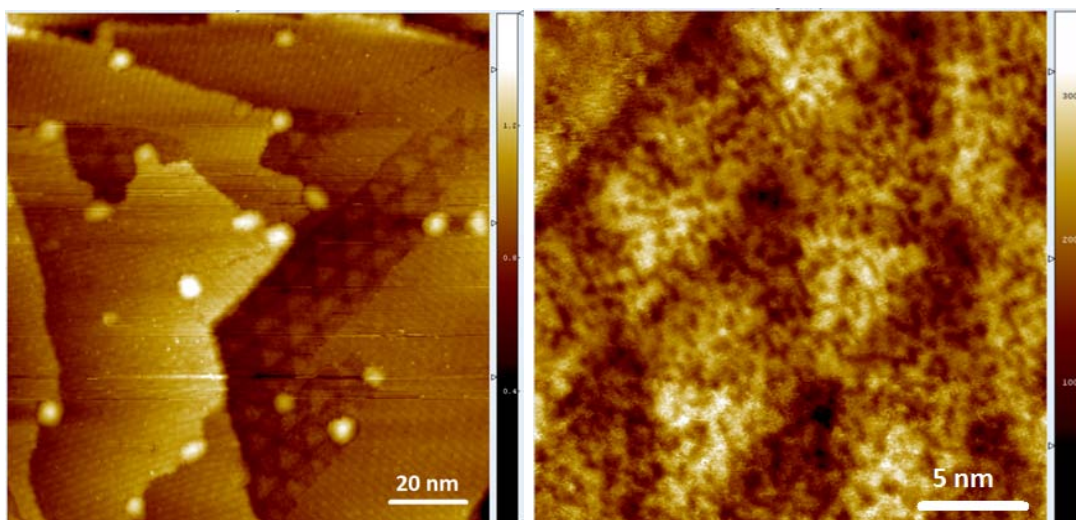


**Figure 2-1:** *STM images of zirconium surface at its early oxidation stage*

anodes. In their paper, Antlanger et. al. combined scanning tunneling microscopy (STM), Auger electron microscopy, and DFT to study the growth of ultrathin  $\text{ZrO}_2$  films on superalloy  $\text{Pt}_3\text{Zr}(0001)$  substrate [6]. In this study Antlanger concluded that the oxide trilayer banded rather weakly to the substrate and bonding to the substrate mainly occurs between the Zr atoms in the oxide and the Pt atoms on the substrate's surface. On the same substrate,  $\text{Pt}_3\text{Zr}$ , in a more recent study, Li et. al. examined the growth of an ultrathin zirconia film using High-resolution X-ray Photoelectron Spectroscopy, Temperature-Programmed Desorption, STM and DFT [5]. Li found that while most of the oxidation led to formation of ultra thin trilayer (O-Zr-O) films on the alloy, formation of  $\text{ZrO}_2$  clusters was also observed, which amount decreased with increasing annealing temperature. On a similar substrate,  $\text{Pd}_3\text{Zr}$ , Choi et. al. suggested that the growth of ultra-thin film  $\text{ZrO}_2$  resulted in a very large superstructure cell [4]. This study also suggested that oxide film binds to the substrate mainly via bonds between oxygen and the Zr atoms in the substrate. In addition, the ultra-thin oxide showed large buckling in STM, which later confirmed by DFT calculations.

From the works that had been mentioned, it could be concluded that using first-principles calculations to study the growth of ultra-thin layer of  $\text{ZrO}_2$  on top of

Zr was feasible. However, since there was a mismatch between zirconium's lattice parameter and that of zirconia, in order to reproduce a stress-free model that was also periodically repetitive along x and y axes, a rather large supercell was needed. A full simulation on a supercell of that size would be too computational expensive. To overcome this kind of problem, many previous studies on different materials had chosen to go with the method of simulations of several smaller models that represented local interface structure [4, 5, 6]. One would have two approaches with this method: one was to use an in-plane lattice spacing for the oxide close to the experimental one but expanding the substrate in x and y (allowing it to contract vertically), and the other one was to keep the substrate lattice constants, which leads to an in-plane compression of the oxide lattice. While an expanded substrate would be, in most cases, more reactive than usual, many of the studies reported to find qualitatively similar results from two different approaches [4].



# Chapter 3

## Computational Methods, Results and Discussion

The DFT calculations in this study were done with the Vienna Ab-initio Simulation Package, which uses a projector augmented-wave formalism to describe the interactions between atoms [10, 11]. An energy cutoff of 450 eV and fine  $\Gamma$ -centered k-point meshes automatically generate with the Monkhorst-Pack scheme [12] ensured electronic convergence of the calculations. To determine the optimum structures, relaxation was done until the residual forces were below 0.01 eV  $\text{\AA}^{-1}$ . In all calculations, the generalized gradient approximation (GGA) as proposed by Perdew, Burke and Ernzerhof [13] (PBE) was used to treat the electronic exchange and correlation effects. For the surface calculations, 10  $\text{\AA}$  of vacuum was placed between the periodic repetitions.

This study consists of two main parts. The first part of this study was to model the substrate zirconium. The second part consisted of calculations that modeled zirconia, the oxide that formed on top of the substrate and calculations that modeled the interaction between the substrate and the oxide models. That substrate/oxide interface, which represented the early phase of zirconium corrosion, was simply formed

by putting the oxide model on top of the substrate model found in the first calculation set.

## 3.1 Zirconium substrate modeling

In order to construct the substrate model, the zirconium slab, two sets of calculations had been done: one on the bulk structure and the other one on the surface structure of zirconium.

### 3.1.1 Zirconium bulk structure

The foremost calculation, that was done in prior to obtaining an acceptable model for bulk zirconium, was to determine a cut-off for the needed size of k-point mesh. On a  $1 \times 1 \times 1$  hexagonal close packed (hcp) cell consisting of two zirconium atoms, several calculations were done using k-point meshes with sizes of  $12 \times 12 \times 8$ ,  $16 \times 16 \times 10$ ,  $20 \times 20 \times 14$ ,  $24 \times 24 \times 16$ ,  $28 \times 28 \times 18$  and  $32 \times 32 \times 20$  with the use of 95, 180, 352, 549, 800 and 1122 irreducible k-points, respectively. The results of those calculations were shown in Fig. 3-1. In this figure, the total energies of the two atoms hcp Zr cells were plotted against the sizes of the k-point mesh used. Using a general convergence cut-off of 5 meV/atom, it was shown that the choice of  $20 \times 20 \times 14$  k-point mesh would be sufficient to represent the zirconium  $1 \times 1 \times 1$  supercell while keeping the computational effort at the minimum level. In subsequent calculations, choice of k-point mesh would be made based on the ratio between the size of the new supercell and that of the  $1 \times 1 \times 1$  supercell.

In the next step, using the chosen k-point mesh in the last part, equation of state calculations were done to determine the computational lattice parameters of bulk zirconium. The procedure was to get the energy as a function of volume using by regression fitting DFT results to third-order Birch-Murnagahn equation of state

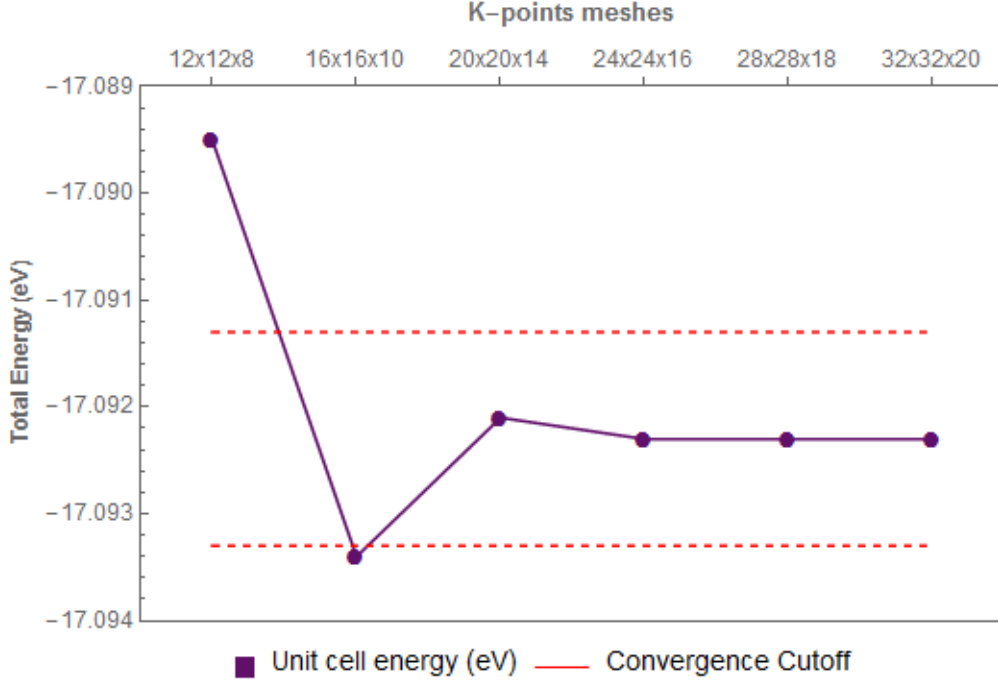


**Figure 3-1:** *Zirconium Metal Bulk K-points convergence*

shown in Eqn. 3.1 [14].

$$E(V) = E_0 + \frac{9V_0B_0}{16} \left\{ \left[ \left( \frac{V_0}{V} \right)^{2/3} - 1 \right]^3 B'_0 + \left[ \left( \frac{V_0}{V} \right)^{2/3} - 1 \right]^2 \left[ 6 - 4 \left( \frac{V_0}{V} \right)^{2/3} \right] \right\} \quad (3.1)$$

The value of  $V_0$  in the equation, which was found from the regression fitting in Fig. 3-2, would be the cell volume that result in the lowest possible total system energy. One last calculation to calculate the Zr lattice parameter was to optimize the ionic structure of a zirconium hcp cell with a fixed volume equal to the value of  $V_0$ . In addition, by getting the energy as a function of volume using third-order Birch-Murnagahn equation of state, information about bulk modulus was also found. Table. 3.1 showed a comparison of the optimized Zr lattice parameters and bulk modulus to the reported experimental values in the literature.

Overall, the zirconium lattice parameter agreed well with previous experiments [14] and DFT calculations [15]. The comparison showed that the predicted geometries of the GGA (PBE) slightly overestimated the experimental lattice parameters, which

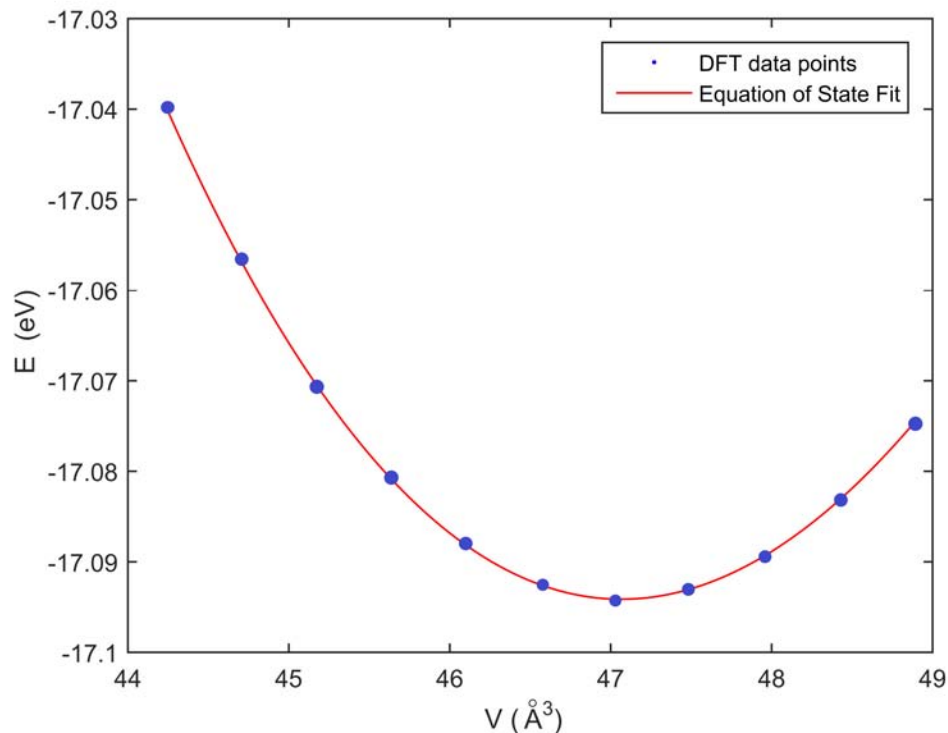


**Figure 3-2:** Regression fitting of DFT results to third-order Birch-Murnagahn equation of state

resulted in an overestimation of the volume by about 1.2%. However, this discrepancy between the DFT results and the reported experimental values was acceptable for this study. Therefore, the current set up of zirconium supercell alongside with the chosen k-points mesh was determined to be approximately accurate in representing the actual zirconium metal structure.

**Table 3.1:** Comparison of the optimized Zr lattice parameters and bulk modulus to the reported experimental values

Parameters	DFT results	Experimental values
a ( $\text{\AA}$ )	3.24	3.233 [16], 3.229 [17], 3.232 [18]
c ( $\text{\AA}$ )	5.17	5.146 [16], 5.141 [17], 5.147 [18]
V ( $\text{\AA}^3$ )	47.07	46.57 [16], 46.44 [17]
B (GPa)	93.8	92 [16]

### 3.1.2 Zirconium surface structure

For the purpose of this study, the only surface direction reproduced was (0001) direction. The Zr (0001) surface was modeled by a periodic slab that consisted of a number of Zr layers separated by a vacuum region, which had a thickness equivalent to that of four bulk Zr layers (10.34 Å). All the atoms were allowed to move. To determine the smallest reasonable size of the surface that could represent the actual Zr (0001) surface well, a series of calculation was carried in which the number of Zr layers was varied from three to seven. An additional calculation, which tried to resemble the zirconium surface set up described in a paper published by Wang et. al. [19], was also done.

**Table 3.2:** *Zirconium surface energies calculated in DFT. Comparison with experimental values is also given.*

	Surface energy (eV/atom)
3 layers	0.907
4 layers	0.912
5 layers	0.894
6 layers	0.904
7 layers	0.900
Wang et. al.	0.901
Experiment	0.81-1.05 [20]

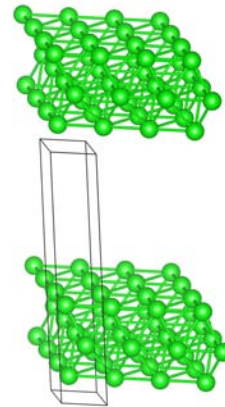


**Figure 3-3:** *A periodic slab that consisted of three zirconium layers separated by a vacuum region, which had a thickness equivalent to that of four bulk Zr layers. The rectangular box represents the actual computational supercell.*

Since accurate experimental values for the surface formation energies of Zr were not available, comparison with experiment was rather a difficult task. However, one good work-around method was to approximate values of Zr surface formation energy by extrapolating from the liquid metal energies and from the heats of vaporization [20]. Table. 3.2 shown zirconium surface energies calculated in DFT and its comparison to values reported in literature. According to this comparison, DFT values of surface

formation energy of zirconium were in a great agreement with reported values from experimental study [20], with a discrepancy of about  $\pm 11\%$ . One important key result from this comparison was that a periodic slab that consisted of three of Zr layers, which shown in Fig. 3-3, was sufficient to represent the zirconium surface structure. Thus, it was chosen to be the substrate model which would then be used to construct zirconium/zirconia interface in Sec. 3.2.

## 3.2 Early phase of zirconium corrosion modeling

At this point, the only missing piece to constructing the metal/oxide interface was the oxide component. For the purpose of this study, the oxide consisted of an O-Zr-O trilayer, equivalent to a (111) trilayer of the fluorite structure of cubic  $\text{ZrO}_2$ . The construction of the oxide trilayer was mostly based on the work that Mostafa et. al. has done previously [21]. In fact, the zirconia bulk structure provided by Mostafa was fully relaxed with the same DFT parameters used in Sec. 3.1. The final zirconia bulk structure was then cut along the (111) surface to prepare the oxide trilayer for the interface modeling.

The Zr/ $\text{ZrO}_2$  interface was modeled by a periodic slab that consisted of one trilayer  $\text{ZrO}_2$  atop of three Zr layers, separated by a vacuum region, which had a thickness equivalent to that of four bulk Zr layers (10.34 Å). All the atoms were allowed to move except the Zr atoms at the bottom-most layer of the substrate. As stated in Chapter. 2, instead of modeling a full size metal/oxide interface along x and y axes, this study would examine the interface at three specific configurations, which were shown in Fig.3-4, 3-5 and 3-6.

All three structures were energetically optimized. DFT calculations showed that the interaction between the oxide and the substrate induced a slight vertical contraction of the oxide film and a slight buckling of the Zr layer in the oxide. While it was observed in ABCA and ABCB configurations that bonding to the substrate

mainly occurred via the Zr atoms in the oxide trilayer, in ABCC configuration, the oxide trilayer bonded to substrate mainly via the O atoms at the bottom layer. In addition, while the Zr atoms in the oxide trilayer in configuration ABCA bonded to two Zr atoms on the substrate surface, those in configuration ABCB only bonded to one Zr atom. Because of those differences, the Zr layer in configuration ABCA buckled downward 25.4 pm more than oxide trilayer in configuration ABCB and 54.9 pm more than oxide trilayer in configuration ABCC. DFT calculations also showed that the buckling effect was more significant than the contraction effect. Oxide trilayer in configuration ABCC contracted vertically 0.58 pm less than oxide trilayer in configuration ABCB and 0.33 pm more than oxide trilayer in configuration ABCA.

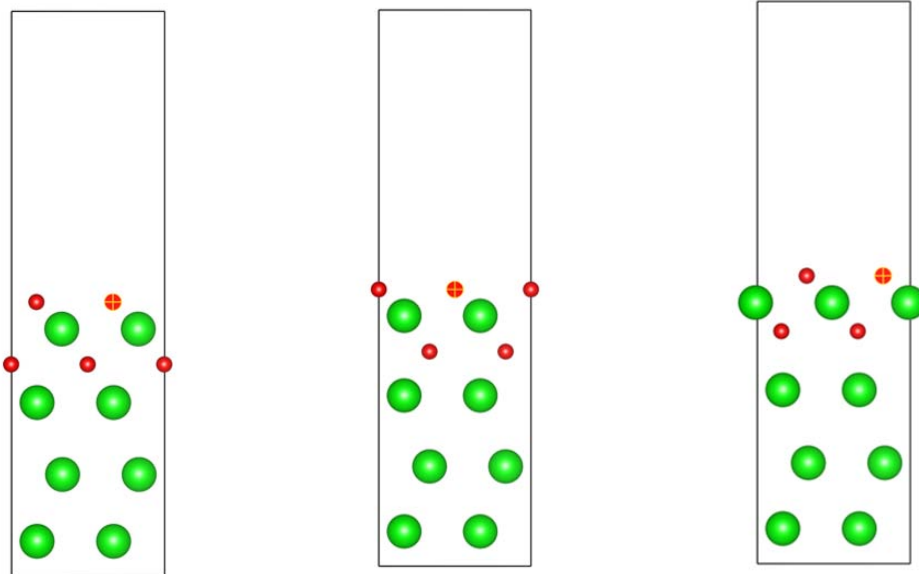


**Figure 3-4:** *Zirconium/zirconia surface with ABCA stacking order*      **Figure 3-5:** *Zirconium/zirconia surface with ABCB stacking order*      **Figure 3-6:** *Zirconium/zirconia surface with ABCC stacking order*

That results indicated that the surface of Zr metal during its initial oxidation stage would be at different heights which were the results of the changes in the buckling of Zr layer in the oxide trilayer. Notice that, the buckling of Zr layer in the oxide trilayer was shown to depend on its relative position to the underneath Zr layer of the substrate's surface. As mentioned previously, since there was a mismatch between Zr metal and  $\text{ZrO}_2$  oxide lattice parameters, the relative position of the oxide

layer and the Zr layer on the substrate's surface will be shifted periodically along x and y axes. Thus the buckling effect combined with the lattice mismatch could be the reason why the repetitive triangle patterns were found in Ma's STM images [22].

# Chapter 4

## Conclusion & Future Work

DFT calculations indicated that many relaxation patterns would be observed on the surface of zirconium at the initial stage of its oxidation. The diversity in relaxation patterns were mostly due to the fact that the Zr layer in the oxide trilayer buckled differently depends on its relative position to the position of the Zr on the substrate surface. Among the three examined configurations, the difference in heights across the oxide surface could reach  $0.55 \text{ \AA}$ . In addition, since there was a mismatch between Zr metal and  $\text{ZrO}_2$  oxide lattice parameters, the relative position of the oxide layer and the Zr layer on the substrate's surface will be shifted periodically along x and y axes. Thus the relaxation patterns will also be periodical along the oxide surface. This could explain the strange patterns found in Ma's STM images [22].

In order to be more precise at comparing the DFT results to the experiment results, calculations for many other different configurations rather than the existing three are needed. To further compare the results from DFT calculations to experimental findings in Ma's reports [22], the three energetically optimized structures could be used to generate STM images. While generating STM images from DFT results is not impossible, only a few literature studies report reliable methods to do so. In his papers [7, 8], Vanpoucke reported to efficiently generate accurate STM images based

on the Tersoff-Hamann method [9] using his software named HIVE-STM. Vanpoucke stated that since according to Tersoff and Hamann, the tunneling-current in an STM experiment was equivalent with the local density of states, it must be reasonable that a surface of constant current in an STM experiment could be identified with a surface of constant density of states in calculations. However, generating STM images from three different calculations could be meaningless since gray-scale shown in those images represented different depths. This meant those three STM images generated represented three different STM experiments with different set up at three positions on the sample's surface rather than one consistent STM experiment. In order to make these DFT-generated images useful, one universal gray-scale must be used across all three images.

In the future, by combining new results at many different configurations along with the STM images generation method, one single STM image of the same size with the STM images gotten from experiment would be possible. At that point, comparing DFT results to experimental results would be most precise.

In addition, as Ma reported in his latest work [22], the surface of the oxide layer is highly defective, which defects seem to be mostly oxygen vacancies. Introducing oxygen vacancy into this study which might lead to more comprehensive results and conclusions could be the next step of this project.

# Bibliography

- [1] Nguyen Q. Minh. Ceramic Fuel Cells. *Journal of the American Ceramic Society*, 76(3):563–588, March 1993.
- [2] B. Cox. Some thoughts on the mechanisms of in-reactor corrosion of zirconium alloys. *Journal of Nuclear Materials*, 336(2-3):331–368, February 2005.
- [3] Bing Li, A.R. Allnatt, C.-S. Zhang, and P.R. Norton. Model and theory for the determination of diffusion coefficients by Auger electron spectroscopy measurements and an application to oxygen diffusion along the [0001] and [101 $\hat{A}$ <sup>-0</sup>] axes in single crystal zirconium. *Surface Science*, 330(3):276–288, June 1995.
- [4] J I J Choi, W Mayr-Schmölzer, F Mittendorfer, J Redinger, U Diebold, and M Schmid. The growth of ultra-thin zirconia films on Pd3Zr(0001). *Journal of physics. Condensed matter*, 26(22):225003, 2014.
- [5] Hao Li, Joong-Il Jake Choi, Wernfried Mayr-Schmölzer, Christian Weilach, Christoph Rameshan, Florian Mittendorfer, Josef Redinger, Michael Schmid, and Günther Rupprechter. Growth of an Ultrathin Zirconia Film on Pt3Zr Examined by High-Resolution X-ray Photoelectron Spectroscopy, Temperature-Programmed Desorption, Scanning Tunneling Microscopy, and Density Functional Theory. *The Journal of Physical Chemistry C*, 119(5):2462–2470, February 2015.
- [6] Moritz Antlanger, Wernfried Mayr-Schmölzer, Ji\ifmmode \checkr\else \vr\fi Pavelec, Florian Mittendorfer, Josef Redinger, Peter Varga, Ulrike Diebold, and

- Michael Schmid. Pt<sub>3</sub>Zr(0001): A substrate for growing well-ordered ultrathin zirconia films by oxidation. *Phys. Rev. B*, 86(3):35451, July 2012.
- [7] Danny Eric Paul Vanpoucke. *Ab initio study of Pt induced nanowires on Ge(001)*. PhD thesis, Enschede, September 2009.
- [8] Danny E P Vanpoucke and Geert Brocks. Formation of Pt-induced Ge atomic nanowires on Pt/Ge(001): A density functional theory study. *Phys. Rev. B*, 77(24):241308, June 2008.
- [9] J Tersoff and D R Hamann. Theory of the scanning tunneling microscope. *Phys. Rev. B*, 31(2):805–813, January 1985.
- [10] G. Kresse. From ultrasoft pseudopotentials to the projector augmented-wave method. *Physical Review B*, 59(3):1758–1775, January 1999.
- [11] Peter E Blöchl, O Jepsen, and O K Andersen. Improved tetrahedron method for Brillouin-zone integrations. *Phys. Rev. B*, 49(23):16223–16233, June 1994.
- [12] Hendrik J Monkhorst and James D Pack. Special points for Brillouin-zone integrations. *Phys. Rev. B*, 13(12):5188–5192, June 1976.
- [13] John P Perdew, Kieron Burke, and Matthias Ernzerhof. Generalized Gradient Approximation Made Simple. *Phys. Rev. Lett.*, 77(18):3865–3868, October 1996.
- [14] Francis Birch. Finite Elastic Strain of Cubic Crystals. *Phys. Rev.*, 71(11):809–824, June 1947.
- [15] Bao Tian Wang, Peng Zhang, Han Yu Liu, Wei Dong Li, and Ping Zhang. First-principles calculations of phase transition, elastic modulus, and superconductivity under pressure for zirconium. *Journal of Applied Physics*, 109(6):0–7, 2011.
- [16] Yusheng Zhao, Jianzhong Zhang, Cristian Pantea, Jiang Qian, Luke L Daemen, Paulo A Rigg, Robert S Hixson, George T Gray, Yunpeng Yang, Liping Wang,

- Yanbin Wang, and Takeyuki Uchida. Thermal equations of state of the  $\alpha\{\}$ ,  $\beta\{\}$ , and  $\omega\{\}$  phases of zirconium. *Phys. Rev. B*, 71(18):184119, May 2005.
- [17] J Goldak, L T Lloyd, and C S Barrett. Lattice Parameters, Thermal Expansions, and Grüneisen Coefficients of Zirconium, 4.2 to 1130K. *Phys. Rev.*, 144(2):478–484, April 1966.
- [18] J C Jamieson. Zirconium: phases and compressibility to 120 kilobars. *High Temperatures-High Pressures*, 5:123–131, 1973.
- [19] X. Wang, M. Khafizov, and I. Szlufarska. Effect of surface strain on oxygen adsorption on Zr (0 0 0 1) surface. *Journal of Nuclear Materials*, 445(1-3):1–6, 2014.
- [20] L E Murr. Interfacial phenomena in metals and alloys. 1975.
- [21] Mostafa Youssef and Bilge Yildiz. Intrinsic point-defect equilibria in tetragonal ZrO<sub>2</sub> : Density functional theory analysis with finite-temperature effects. *Physical Review B*, 86(14):144109, October 2012.
- [22] Wen Ma. Initial surface oxide structure during early stages of zirconium oxidation. 2015.

MIT OpenCourseWare  
<http://ocw.mit.edu>

## 22.THT Undergraduate Thesis Tutorial

Fall 2015

For information about citing these materials or our Terms of Use, visit: <http://ocw.mit.edu/terms>.